JOURNAL OF GEOPHYSICAL RESEARCH, VOL. 95, NO. A6, PAGES 8243–8251, JUNE 1, 1990

A Solar EUV Flux Model

W. KENT TOBISKA[1]

Cooperative Institute for Research in Environmental Sciences, National Oceanic and Atmospheric Administration University of Colorado, Boulder

CHARLES A. BARTH

Laboratory for Atmospheric and Space Physics, University of Colorado, Boulder

A model of the solar extreme ultraviolet (EUV) irradiance variability has been developed for aeronomical use and has been named SERF2 by the Solar Electromagnetic Radiation Flux Study. The model is valid between 1981 and 1989 and is based on the Atmosphere Explorer E (AE-E) satellite EUV data set which is correlated with independent solar emissions measured during and after the AE-E mission. Additionally, spectral modifications are made to the model based on 18 separate rocket flights for all levels of solar activity. Two daily measured solar emissions, the H Lyman α line at 121.6 nm observed by the Solar Mesosphere Explorer satellite and the Ottawa 10.7-cm radio flux observed at the ground, are used in the model as indices for full-disk solar EUV chromospheric irradiance variations and transition region–coronal irradiance variations, respectively. The model wavelength equation coefficients are presented in tabular form for 39 wavelength groups or discrete lines from 1.9 to 105.0 nm along with spectral weighting function coefficients which modify the irradiance magnitudes based upon model wavelength fits to rocket-observed spectra. The model satisfies the general constraint of duplicating rocket-observed EUV irradiance for a wide variety of solar activity conditions. The model development is discussed, an example calculation is given, and the comparisons with constraining rocket data sets are shown.

INTRODUCTION

The upper atmosphere of the Earth is of great interest to a number of scientific and engineering communities. The atmosphere's structure between 100 and 500 km varies in response to solar energy, auroral energy, and tides. The net result of photoabsorption, auroral particle precipitation, and Joule dissipation of ionospheric currents, tides, and atmospheric waves is atmospheric heating. The most significant component in global thermospheric heating is the introduction of energy from EUV and soft X ray wavelengths in the solar electromagnetic spectrum. This spectral range is created in the solar chromosphere, chromosphere-corona transition region, and corona. This flux, consisting of wavelengths shorter than 102.7 nm down to the X rays, is absorbed in the upper atmosphere by the major neutral constituents of O, N_2, and O_2. These emissions are also responsible for the ionization of the E and F regions, and their variation in time is one of the fundamental variables in thermospheric and ionospheric physics.

In the future, direct and instantaneous measurements of thermospheric density, composition, and temperature may become regularly available. However, until consistent monitoring can take place, modeling of the thermosphere will be the primary means of determining and predicting variations in the fundamental characteristics of temperature and density. The current problem of accurately modeling the density and temperature of the thermosphere as it varies with solar activity partially results from the lack of consistently measured solar EUV and soft X ray emissions.

Since EUV wavelengths are entirely absorbed prior to reaching the ground, the only methods of measuring them to the present have been rocket flights and satellite observations. These solar EUV measurements by satellites have been conducted on a daily basis during brief intervals of time: in the late 1960s by the OSO series satellites, in the early 1970s by the AEROS satellites, in the late 1970s by the Atmosphere Explorer (AE) series satellites, by Prognoz 10 in 1985, and by the San Marco satellite in 1988. Future observations may be made of the direct or indirect solar EUV irradiance variations by the absolute, extreme-ultraviolet, solar spectral irradiance monitor (AESSIM) instrument [*Huber et al.*, 1988], SOHO satellite [*Huber et al.*, 1988], and EUVE satellite [*Bowyer*, 1983; Extreme Ultra Violet Explorer Informational Package, Space Astrophysics Group, University of California, Berkeley, 1989]. This paucity of daily data, especially pronounced beginning in the 1980s, has been referred to as "the EUV hole" by *Donnelly* [1987*a*]. Therefore the EUV has mainly been parameterized by indices of solar activity which are observed at the Earth's surface. Zurich sunspot numbers, Rz, and 10.7-cm solar radio flux, $F_{10.7}$, have historically been used as indicators of the general level of solar EUV flux, although neither has any direct influence on the terrestrial atmosphere.

Previous empirical modeling of the solar EUV flux began prior to space-based observations with *Saha* [1937], who suggested an "ultraviolet excess factor" of up to 1×10^6 modification of the solar blackbody spectrum of 6500 K. After EUV measurements were made above the Earth's atmosphere, *Hinteregger et al.* [1965] tabulated what became known as an "EUV flux standard" based on rocket measurements, and *Roble and Schmidtke* [1979] identified typical examples of EUV flux during low and moderate solar

[1]Now at Space Sciences Laboratory, University of California, Berkeley.

Paper number 89JA03304.
0148-0227/90/89JA-03304$05.00

TABLE 1. Data Sets Used in Solar EUV Flux Model

Data Set	Time Period	Use in Model
AE-E Lyman α	July 1, 1977, to Dec. 21, 1978	linear correlation
AE-E EUV	July 1, 1977, to Dec. 21, 1978	linear correlation
$F_{10.7}$	July 1, 1977, to Dec. 21, 1978	linear correlation
$F_{10.7}$	Jan. 1, 1982, to Aug. 26, 1986	EUV flux index time series
SME Lyman α	Jan. 1, 1982, to Aug. 26, 1986	EUV flux index time series
LASP EUV rocket	Nov. 10, 1988 [*Woods and Rottman*, 1990]	weighting functions for $\lambda > 30.0$ nm
17 EUV rockets	all solar levels [*Feng et al.*, 1989]	weighting functions for $\lambda < 30.0$ nm

conditions for aeronomical applications. *Hinteregger et al.* [1981] developed empirical EUV flux models by using two modeling methods: (1) a two-variable $F_{10.7}$ association formula, using daily $F_{10.7}$ and its 81-day averaged and (2) an EUV class model. The $F_{10.7}$ association model is given for the EUV flux I at a wavelength λ:

$$I_\lambda = A_\lambda F^*_{10.7} + B_\lambda(F_{10.7} - F^*_{10.7}) + C_\lambda \quad \text{photons cm}^{-2}\ \text{s}^{-1} \tag{1}$$

where $F_{10.7}$ is the daily value and $F^*_{10.7}$ is the 81-day mean. A_λ, B_λ, and C_λ are obtained from a least squares fit to the AE-E EUV data. Equation (1) models the EUV flux for time periods other than those covered by the AE-E data set, is reviewed by *Schmidtke* [1984], is now called SERF1, and has been compiled in digital form by the Solar Electromagnetic Radiation Flux Study subgroup of the World Ionosphere-Thermosphere Study (WITS). WITS is an international interdisciplinary program of research organized by the Scientific Committee on Solar-Terrestrial Physics (SCOSTEP) which started July 1, 1987, and continued to December 31, 1989. SERF1 is available from the NOAA National Geophysical Data Center (NGDC).

However, a more accurate representation of EUV flux for the period during the AE-E mission is given by I_λ in the EUV class model,

$$I_\lambda = I_{\lambda\text{ref}} + I_{\lambda\text{ref}}(R_k - 1)C_\lambda \quad \text{photons cm}^{-2}\ \text{s}^{-1} \tag{2}$$

where $I_{\lambda\text{ref}}$ is the EUV flux at solar cycle 21 minimum given by *Hinteregger et al.* [1981]. R_k is the ratio for a specific date of a key EUV flux to the solar minimum value. C_λ is a wavelength-dependent scaling parameter for each EUV wavelength. The two key emissions are a chromospheric emission, Lyman β (102.6 nm), and a coronal emission, Fe XVI (33.5 nm). *Schmidtke* [1984] further reviews the EUV class model along with other methods of representing solar EUV flux for aeronomical applications. Previous work [*Hinteregger et al.*, 1981; *Bossy and Nicolet*, 1981; *Bossy*, 1983; *Hedin*, 1984; *Donnelly et al.*, 1986; *Tobiska and Barth*, 1988*a*] has shown that the AE-E EUV flux may be compared with the $F_{10.7}$. *Tobiska and Barth* [1988*a*] also compared the EUV flux to Lyman α and to the GOES 1- to 8-Å X rays. Conclusions from this body of work indicate that the greatest correlations in the AE-E data set are as follows: the chromospheric EUV emissions are most highly correlated with Lyman α, and the transition region–coronal emissions are most highly correlated with $F_{10.7}$.

This present work introduces solar Lyman α flux combined with $F_{10.7}$ as indices for the full-disk solar EUV irradiance variation. It follows the approach of *Hinteregger et al.* [1981] of estimating the full EUV spectrum using measurements of discrete lines which are created in similar solar source regions. The original indices from *Hinteregger et al.* [1981] of Lyman β and Fe XVI are no longer available on a daily basis. *Tobiska* [1988] and *Tobiska and Barth* [1988*a*] show that the solar Lyman α, measured on a daily basis by the Solar Mesosphere Explorer (SME) [*Rottman et al.*, 1982; *Rottman*, 1987] for $7\frac{1}{2}$ years (G. Rottman, private communication, 1989), and the $F_{10.7}$ emission, measured at the Ottawa observatory since 1947, are useful indices for modeling the dominant EUV and soft X ray emissions. Solar Lyman α is an effective chromospheric EUV emission indicator, and $F_{10.7}$ is an effective transition region and coronal EUV emission indicator. The EUV flux model based on this work has been named SERF2 by the Solar Electromagnetic Radiation Flux Study.

An overview of the modeling details can be summarized. AE-E Lyman α is linearly correlated with solar chromospheric region AE-E EUV flux, and $F_{10.7}$ is linearly correlated with solar transition region and coronal AE-E EUV flux such that least squares coefficients are obtained for the basic model at 39 wavelength intervals or discrete lines. Next, a constraint for the model to reproduce rocket-observed spectra for all levels of solar activity is placed on the model to improve its accuracy. This is accomplished by developing spectral weighting functions which are empirically determined and which enable a match between the model spectrum derived from the AE-E correlations and the spectrum observed by several rockets of discrete lines as well as broadband integrated flux. The complete EUV model is presented in tabular form for ease of use in aeronomical applications. The format of 39 wavelength intervals or discrete lines is the same as the 37 categories outlined by *Torr et al.* [1979] and *Torr and Torr* [1985] with the exception that two intervals in the soft X rays (1.9–3.0 nm and 3.0–4.9 nm) are added to the model.

SOLAR EUV MODEL

Data from five separate sources, comprising seven data sets and spanning over a decade between 1977 and 1988, are used in this study and shown in Table 1. Two particular satellites, the AE-E and SME, have made long-term observations of the solar spectrum and have provided data which are used in this work. Solar radio data from the World Data Center (WDC) are extensively used. Results from 18 EUV rocket flights [*Feng et al.*, 1989; *Woods and Rottman*, 1990] have also been incorporated into this model.

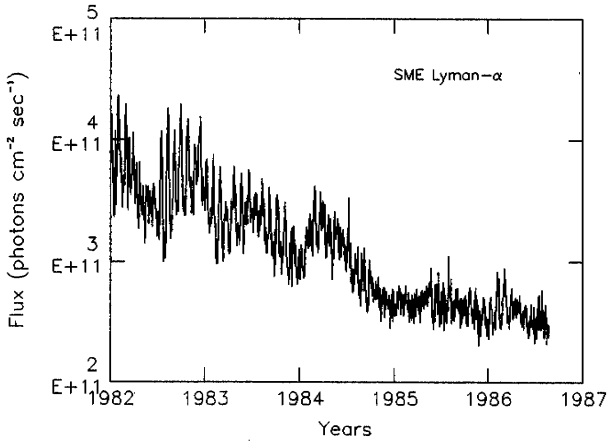

Fig. 1. Three-day smoothed daily averaged SME Lyman α between January 1, 1982, and August 26, 1986.

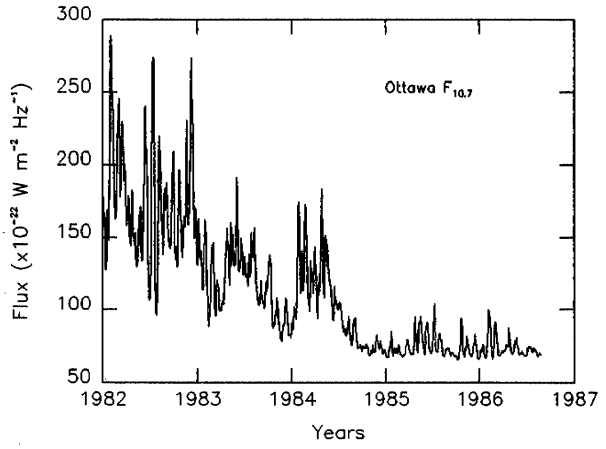

Fig. 2. Daily observed Ottawa 10.7-cm radio emission between January 1, 1982, and August 26, 1986.

Figures 1 and 2 show the model's two indices, SME Lyman α and the Ottawa $F_{10.7}$, for the period of time from January 1, 1982, through August 26, 1986. Both solar emissions show an underlying decline of flux intensity during the decline of cycle 21 to solar minimum with superimposed 27-day solar rotational variations and longer-period intermediate-term variations persisting for several solar rotations. The Lyman α daily minimum is in August 1986, and the $F_{10.7}$ daily minimum is in September 1986.

This model is based on the linear correlations of AE-E Lyman α with the AE-E chromospheric EUV emissions and of $F_{10.7}$ with the AE-E transition region–coronal emissions during the rise of cycle 21 from July 1, 1977, through December 21, 1978. The data during the rise of solar cycle 21 through December 21, 1978, were used in this study for two reasons. First, it was important to select a range of data which demonstrated considerable variation in magnitude in order to sample low, moderate, and high solar activity. Second, there is debate in the literature concerning the source of an apparent abrupt magnitude change of AE-E Lyman α after December 21, 1978 [*Bossy and Nicolet*, 1981; *Bossy*, 1983; *Fukui*, 1988]. Therefore, after December 21, 1978, AE-E Lyman α data were not used for this study.

The coefficients of linear correlation between the data sets for the period of the full AE-E mission (July 1, 1977, through December 30, 1980) have been summarized by *Hedin* [1984] and for the rise of cycle 21 by *Tobiska and Barth* [1988*a*]. These are summarized in Table 2. The important feature in Table 2 is that the Lyman α correlations are highest with the chromospheric EUV emissions and the $F_{10.7}$ correlations are highest with the transition region–coronal EUV emissions. There is a fairly good correlation between all comparisons, one might argue, but the coefficient of correlation has a substantial component which is likely to be influenced by the long-term trends in the data sets (O. R. White, private communication, 1988). For this study, the AE-E Lyman α and $F_{10.7}$ data are smoothed with a 13-day running mean algorithm to remove short-term variations. The smoothed data are then linearly correlated with each of the AE-E 39 wavelength intervals or discrete lines listed in Tables 3 and 4.

TABLE 2. Linear Correlation Coefficients for AE-E Data

Wavelength Interval, Å	Solar Source Region*	Correlation With Lyman α†	Correlation With $F_{10.7}$†	Correlation With $F_{10.7}$‡
168–190	T, CC	0.80	0.89	0.84
169–173	T	0.77	0.86	0.82
178–183	T, CC	0.80	0.87	0.84
190–206	T, CC	0.81	0.88	0.85
200–204	CC	0.82	0.88	0.85
206–255	Ch + BT, T, CC, HC	0.82	0.91	0.89
255–300	HC, Ch + BT	0.83	0.91	0.90
284	HC	0.85	0.92	0.91
304	Ch + BT	0.85	0.85	0.90
335	HC	0.82	0.95	0.94
510–580	Ch + T	0.89	0.83	0.86
584	Ch + BT	0.89	0.86	0.88
590–660	Ch, T, CC	0.88	0.83	0.85
1026	Ch + BT	0.91	0.89	0.90

*Code adapted from *Donnelly* [1987*b*]: Ch = chromosphere; BT = base of the transition region between the chromosphere and corona; T = chromosphere-corona transition region; CC = cool corona; HC = hot corona.

†From *Tobiska and Barth* [1988*a*] for the period July 1, 1977, through December 21, 1978.

‡From *Hedin* [1984] for the period July 1, 1977, through December 30, 1980.

TABLE 3. Chromospheric Emission Coefficients

Wavelength Interval	Intercept	Slope
18.62–29.52	0.0000E+00	0.0000E+00
30.02–49.22	8.64574E−04	9.60715E−04
50.52–99.99	9.16964E−03	1.01854E−02
100.54–148.40	2.44611E−03	2.36549E−03
150.10–198.58	9.83623E−03	3.80251E−03
200.02–249.18	1.15316E−02	4.47421E−03
256.32–256.32	1.15847E−02	1.65490E−03
284.15–284.15	0.0000E+00	0.0000E+00
251.10–299.50	1.74342E−04	9.66984E−04
303.31–303.31	0.0000E+00	0.0000E+00
303.78–303.78	2.49580E−01	3.56501E−02
303.31–349.85	0.0000E+00	0.0000E+00
368.07–368.07	0.0000E+00	0.0000E+00
356.01–399.82	4.32063E−04	9.68613E−05
401.14–436.70	4.47497E−03	1.00319E−03
465.22–465.22	0.0000E+00	0.0000E+00
453.00–499.37	1.88729E−03	1.78671E−03
500.00–550.00	7.18125E−03	2.78783E−03
554.37–554.37	1.56790E−02	3.23537E−03
584.33–584.33	1.50905E−03	1.30326E−02
554.37–599.60	6.98594E−03	2.30912E−03
609.76–609.76	0.0000E+00	0.0000E+00
629.73–629.73	2.53029E−02	5.49650E−03
609.76–644.10	1.18972E−03	3.45875E−04
650.30–700.00	2.01972E−03	6.84290E−04
703.36–703.36	6.54365E−03	1.12692E−03
701.00–750.00	8.78830E−04	8.35838E−04
765.15–765.15	2.22136E−03	7.39790E−04
770.41–770.41	0.0000E+00	0.0000E+00
787.71–787.71	3.83174E−03	7.90574E−04
750.01–800.00	1.23617E−02	4.91086E−03
801.00–850.00	9.98898E−03	9.10774E−03
851.00–900.00	1.63340E−03	2.46990E−02
901.00–950.00	7.98482E−03	2.06026E−02
977.02–977.02	4.86867E−02	1.80840E−02
951.00–1000.00	1.00441E−02	6.61423E−03
1025.70–1025.70	1.37646E−03	2.08082E−02
1031.90–1031.90	−1.47633E−03	1.56699E−02
1001.00–1050.00	1.82233E−02	1.30975E−02

Intercept and slope coefficients in the equation $E_\lambda = a + bw_{chr}$(Lyman α) where SME Lyman α is in ergs per square centimeter per second and is smoothed with a 13-day running mean algorithm. Read 8.64574E−04 as 8.64574×10^{-4}.

The 39 wavelength intervals or discrete lines are formed in the following manner. Each of the several hundred lines in the spectral range of 1.9–105.0 nm is classified as chromospheric or transition region–coronal in origin according to the *Hinteregger et al.* [1981] method of key = 1 or key = 2, respectively, used in the AE-E EUV solar minimum reference spectrum SC#21REFW. The full range of EUV lines are recreated in a time series from the method summarized in equation (2) above. The line intensities are summed to form intensities integrated over an interval where necessary. In cases where discrete lines are listed separately in Tables 3 and 4, these lines are not included in the intervals. The EUV calculated irradiance time series from equation (2) are then smoothed with the 13-day running mean, and a correlation is performed with either AE-E Lyman α or $F_{10.7}$ depending upon their chromospheric or transition region–coronal origin, respectively. The resulting intercept and slope coefficients are listed in Tables 3 and 4 for the chromospheric and transition region–coronal energy flux.

After the wavelength coefficients are obtained from the AE-E data comparisons, the model is next extended to the post–AE-E period. SME Lyman α and $F_{10.7}$ from 1981–1989 are used to do this. In order to create EUV flux which is representative of given solar conditions for time periods beyond the correlation time interval, the chromospheric and transition region–coronal energy flux time series are first created from the coefficients in Tables 3 and 4 using the input indices of 13-day smoothed SME Lyman α or $F_{10.7}$, respectively. Then the modeled EUV flux is modified with spectral weighting functions which have been empirically determined to adjust the model results at each wavelength to the observed EUV flux by rocket flights. These functions, w_1, w_2, and w_{chr}, enable the model to spectrally match the November 10, 1988, Laboratory for Atmospheric and Space Physics (LASP) EUV rocket flight [*Woods and Rottman*, 1990] and spectrally approximate the integrated soft X ray and EUV flux from 17 rocket flights during diverse solar activity conditions which are reviewed by *Feng et al.* [1989]. The empirically determined weighting functions are applied to the calculations of the chromospheric and transition region–coronal energy fluxes separately before summing both components into a full-disk modeled interval flux.

The chromospheric energy flux is calculated and modified by

TABLE 4. Transition Region and Coronal Emission Coefficients

Wavelength Interval	Intercept	Slope
18.62–29.52	−1.79720E−02	3.18809E−04
30.02–49.22	−1.77202E−02	3.40050E−04
50.52–99.99	−6.42898E−03	7.99157E−04
100.54–148.40	3.26442E−03	8.74992E−05
150.10–198.58	1.27261E−02	2.38466E−03
200.02–249.18	−5.92997E−02	1.54553E−03
256.32–256.32	0.0000E+00	0.0000E+00
284.15–284.15	−9.36616E−02	1.39477E−03
251.10–299.50	−6.51540E−02	1.70927E−03
303.31–303.31	−4.97807E−02	9.03115E−04
303.78–303.78	0.0000E+00	0.0000E+00
303.31–349.85	−7.40308E−02	1.74077E−03
368.07–368.07	2.58679E−02	2.05401E−04
356.01–399.82	−3.80497E−02	6.45189E−04
401.14–436.70	8.15105E−04	1.29010E−04
465.22–465.22	4.49212E−03	4.58682E−05
453.00–499.37	−1.42005E−02	2.37533E−04
500.00–550.00	−5.78278E−03	9.88009E−05
554.37–554.37	0.0000E+00	0.0000E+00
584.33–584.33	0.0000E+00	0.0000E+00
554.37–599.60	0.0000E+00	0.0000E+00
609.76–609.76	1.72306E−04	2.00784E−04
629.73–629.73	0.0000E+00	0.0000E+00
609.76–644.10	−5.26566E−04	4.56454E−05
650.30–700.00	1.32153E−03	7.12330E−06
703.36–703.36	0.0000E+00	0.0000E+00
701.00–750.00	0.0000E+00	0.0000E+00
765.15–765.15	0.0000E+00	0.0000E+00
770.41–770.41	1.39946E−03	6.72645E−05
787.71–787.71	0.0000E+00	0.0000E+00
750.01–800.00	7.40834E−04	3.56129E−05
801.00–850.00	0.0000E+00	0.0000E+00
851.00–900.00	0.0000E+00	0.0000E+00
901.00–950.00	0.0000E+00	0.0000E+00
977.02–977.02	0.0000E+00	0.0000E+00
951.00–1000.00	0.0000E+00	0.0000E+00
1025.70–1025.70	0.0000E+00	0.0000E+00
1031.90–1031.90	0.0000E+00	0.0000E+00
1001.00–1050.00	0.0000E+00	0.0000E+00

Intercept and slope coefficients in the equation $E_\lambda = a + b(w_1 F_{10.7mod} + w_2 F_{10.7})$ where $F_{10.7}$ is in $\times 10^{-22}$ W m^{-2} Hz^{-1} and is smoothed with a 13-day running mean algorithm. Read −1.79720E−02 as -1.79720×10^{-2}.

TABLE 5. Weighting Values for EUV Emissions

Wavelength Interval	w_1	w_2	w_{chr}
18.62–29.52	0.00000	2.00000	1.0000
30.02–49.22	0.24000	1.76000	1.0000
50.52–99.99	0.80000	1.20000	1.0000
100.54–148.40	1.12500	1.12500	1.0000
150.10–198.58	1.12500	1.12500	1.0000
200.02–249.18	0.33750	1.91250	1.0000
256.32–256.32	0.00000	0.00000	1.0000
284.15–284.15	0.00000	1.05000	1.0000
251.10–299.50	0.18000	2.07000	1.0000
303.31–303.31	0.00000	1.17450	1.0000
303.78–303.78	0.00000	0.00000	0.5873
303.31–349.85	0.00000	1.38080	1.7260
368.07–368.07	0.00000	0.01272	0.0254
356.01–399.82	0.02037	1.20180	1.0184
401.14–436.70	0.24172	0.44890	3.4531
465.22–465.22	0.00000	1.04710	0.8055
453.00–499.37	0.29122	0.65524	0.7281
500.00–550.00	1.23810	0.56275	2.2510
554.37–554.37	0.00000	0.00000	0.5841
584.33–584.33	0.00000	0.00000	0.5258
554.37–599.60	0.00000	0.00000	1.6545
609.76–609.76	0.00000	0.42239	0.5280
629.73–629.73	0.00000	0.00000	0.6448
609.76–644.10	5.40850	3.60570	1.2019
650.30–700.00	2.22570	0.74191	2.4730
703.36–703.36	0.00000	0.00000	0.8529
701.00–750.00	0.00000	0.00000	2.8459
765.15–765.15	0.00000	0.00000	2.8179
770.41–770.41	0.00000	1.80570	1.2038
787.71–787.71	0.00000	0.00000	10.930
750.01–800.00	0.00000	0.00000	0.0000
801.00–850.00	0.00000	0.00000	1.9197
851.00–900.00	0.00000	0.00000	1.5441
901.00–950.00	0.00000	0.00000	1.5157
977.02–977.02	0.00000	0.00000	1.0000
951.00–1000.00	0.00000	0.00000	0.9826
1025.70–1025.70	0.00000	0.00000	1.0737
1031.90–1031.90	0.00000	0.00000	2.0631
1001.00–1050.00	0.00000	0.00000	0.0497

$$E_{\lambda chr} = a_1 + b_1 w_{chr} F_{Ly\alpha} \quad \text{ergs cm}^{-2}\ \text{s}^{-1} \tag{3}$$

where the subscript 1 refers to the intercept and slope coefficients in Table 3, $F_{Ly\alpha}$ is the 13-day smoothed SME Lyman α flux in ergs per square centimeter per second, and w_{chr} is a wavelength-dependent chromospheric weighting function whose values for each of the 39 wavelength intervals are listed in Table 5, last column. The average value of w_{chr} across all wavelengths, $\overline{w_{chr}} = 1.46$, corresponds to the approximate factor by which the solar minimum SME Lyman α must be multiplied in order to raise it to the AE-E Lyman α solar minimum value. Solar cycle 20 minimum (July 1976) for AE-E Lyman α is 3×10^{11} photons cm^{-2} s^{-1}, while solar cycle 21 minimum (August 1986) for SME Lyman α is 2.3×10^{11} photons cm^{-2} s^{-1}. This does not judge the AE-E nor the SME Lyman α calibrations. However, since the model correlations were made with the AE-E Lyman α data, the SME Lyman α should be scaled to the approximate AE-E values for modeling purposes. The w_{chr} function accomplishes this goal across the entire EUV spectrum along with allowing a spectral line fit between the model and the rocket data. w_{chr} is derived using an iterative technique. This technique computationally converges to a weighting value for the modeled chromospheric flux in each interval or at each line such that there is less than 1% difference between the final model 5.0-nm bin value and the November 10, 1988, LASP rocket 5.0-nm bin value where the model uses the $F_{10.7}$ and Lyman α on that date for the initial flux calculation.

The transition region–coronal energy flux is calculated and modified by

$$E_{\lambda cor} = a_2 + b_2(w_1 F_{10.7mod} + w_2 F_{10.7}) \quad \text{ergs cm}^{-2}\ \text{s}^{-1} \tag{4}$$

where the subscript 2 refers to the intercept and slope coefficients in Table 4. w_1 and w_2 are wavelength-dependent transition region–coronal weighting functions whose values for each of the 39 wavelength intervals are listed in Table 5, second and third columns, respectively; w_1 and w_2 are empirically determined in a manner similar to that used for w_{chr}. $F_{10.7}$ in this equation is the 13-day smoothed $F_{10.7}$ value while $F_{10.7mod}$ is a pseudo-$F_{10.7}$ based upon the SME daily average Lyman α value correlated to $F_{10.7}$ during the decline of solar cycle 21. Here

$$F_{10.7mod} = -218.88 + 1.05453 \times 10^{-9}\text{Lyman } \alpha \tag{5}$$

where Lyman α in (5) is in photons cm^{-2} s^{-1}. $F_{10.7mod}$, as given in (5), is used both as an abbreviation within (4) and for empirical reasons. The latter reason is based on the assumption that there is a transition region component to $F_{10.7}$ that varies somewhat differently from the observed flux which comes from several source regions but which is strongly influenced by coronal emission. The $F_{10.7}$ index is split into two components, $F_{10.7mod}$ and $F_{10.7}$, in order to empirically weight the transition region–coronal flux with a temporal variation which has some similarity to chromospheric variations. This motivation is further discussed below.

The chromospheric and transition region–coronal components are both summed to give a total full-disk energy flux for that wavelength interval or discrete line from the method

$$E_\lambda = E_{\lambda chr} + E_{\lambda cor} \quad \text{ergs cm}^{-2}\ \text{s}^{-1} \tag{6}$$

This constitutes the solar EUV flux model.

An example of the model calculation of an EUV flux for given solar activity is as follows. If $F_{10.7} = 158.2 \times 10^{-22}$ W m^{-2} Hz^{-1} and Lyman $\alpha = 5.9 \times 10^{11}$ photons cm^{-2} s^{-1}, the energy flux for the mixed wavelength interval between 200.02 and 249.28 Å can be determined. The chromospheric energy fluxes from (3) in the interval are

$$E_{200-249chr} = 1.15316 \times 10^{-2} + (4.47421 \times 10^{-3})(1.0)(9.6421)$$
$$= 5.4672 \times 10^{-2} \quad \text{ergs cm}^{-2}\ \text{s}^{-1}$$

where

$$9.6421 = \frac{(5.9 \times 10^{11})(12{,}400)(1.602192 \times 10^{-12})}{1215.67}$$

is the conversion of Lyman α photon flux to energy flux. The transition region–coronal energy fluxes from (4) in the interval are

$$E_{200-249cor} = -5.92997 \times 10^{-2} + (1.54553 \times 10^{-3})[(0.3375)$$
$$\cdot(403.29) + (1.9125)(158.20)] = 0.6187 \quad \text{ergs cm}^{-2}\ \text{s}^{-1}$$

where

$$403.29 = -218.88 + (1.05453 \times 10^{-9})(5.9 \times 10^{11})$$

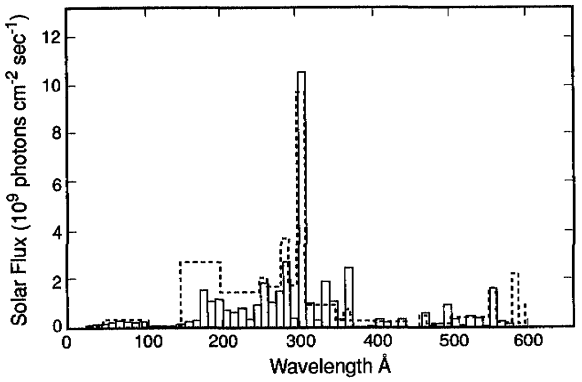

Fig. 5. The composite solar flux reference spectrum (solid line) is taken from *Feng et al.* [1989] and above 75 Å represents the AFGL rocket flight data of August 14, 1979, in 1.0-nm bins. The model (dotted line) consists of 5.0-nm-binned data averaged into 1.0-nm bins for the wavelength intervals listed in Tables 3, 4, and 5 while the discrete line modeled flux from these same tables is added into the appropriate 1.0-nm bin. The model spectrum was created with Lyman $\alpha = 5.9 \times 10^{11}$ photons cm^{-2} s^{-1} and $F_{10.7} = 158.2 \times 10^{-22}$ W m^{-2} Hz^{-1}.

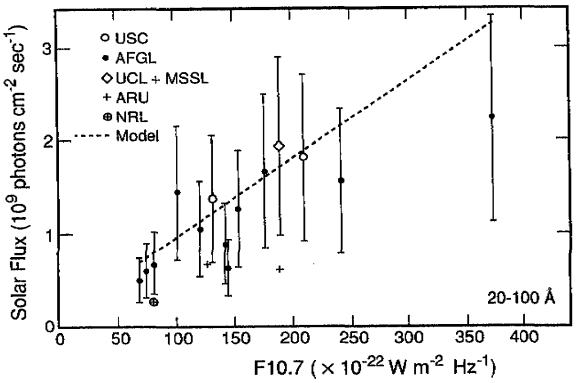

Fig. 6. The integrated solar soft X ray flux between 2.0 and 10.0 nm is taken from *Feng et al.* [1989] (points with error bars). These measurements are from rocket experiments performed by several organizations over a wide range of solar activity with $F_{10.7}$ ranging from 70 to 370. The EUV model estimated flux is shown as the dotted line and is described in the text. The acronyms are USC (University of Southern California), AFGL (Air Force Geophysics Laboratory), UCL (University College London), MSSL (Mullard Space Science Laboratory), ARU (Astrophysics Research Unit at Culham, England), and NRL (Naval Research Laboratory). From Feng et al., all error bars on the measurements are ±50%. The NRL and ARU photographic data have no error bars plotted.

spectrum as well as the integrated flux spectrum for 2.0–10.0 nm and 5.0–57.5 nm for low to high solar activity conditions. Figure 5 shows the Feng et al. composite spectrum as a solid line which is partially based upon the Air Force Geophysics Laboratory (AFGL) rocket experiment on August 14, 1979. The flux in $\times 10^9$ photons cm^{-2} s^{-1} is binned in 1.0-nm intervals. The modeled EUV flux has 5.0-nm bin resolution for each of the wavelength intervals but displayed in 1.0-nm bins where each wavelength interval bin is 20% of the 5-nm bin except for the contribution of discrete lines. The model values are shown as a dotted line in this composite spectrum. In Figure 5, $F_{10.7} = 158.2 \times 10^{-22}$ W m^{-2} Hz^{-1} from the NGDC, and Lyman $\alpha = 5.9 \times 10^{11}$ photons cm^{-2} s^{-1}. The Lyman α value was determined by reducing the AE-E Lyman α observed value of 7.7×10^{11} photons cm^{-2} s^{-1} by the ratio of AE-E to SME for solar minimum (1.3:1). This new Lyman α value is called an equivalent SME Lyman α value. The w_{chr} weighting function then restores the full weighting to the calculated chromospheric flux when used with the equivalent Lyman α. There is fairly good agreement with the important He II (30.4 nm) line as well as most other intervals and discrete lines in this composite spectrum. The apparent exceptions are the disagreements with the 15.0- to 20.0-nm and 20.0- to 25.0-nm intervals and the 36.8-nm line where the model is higher than the Feng et al. spectrum. Possible reasons for this disagreement are summarized below in the discussion on model weaknesses.

Figure 6 shows the Feng et al. 2.0- to 10.0-nm integrated spectrum for 17 rocket experiments from low to high solar activity denoted by $F_{10.7}$ from 70 to 370. The different symbols refer to rocket experiments by separate organizations. The dotted line is the interpolated flux values for seven cases of solar activity where the model was run with $F_{10.7}$ inputs of 70, 120, 170, 220, 270, 320, and 370. Lyman α inputs were 2.7×10^{11}, 3.2×10^{11}, 3.7×10^{11}, 4.2×10^{11}, 4.6×10^{11}, 5.1×10^{11}, and 5.6×10^{11}, respectively, which correspond to the approximate SME Lyman α values derived from the relationship in (5) using the seven $F_{10.7}$ values. The reader is reminded that the w_{chr} weighting function scales the SME Lyman α values to the approximate AE-E Lyman α values. These example cases were also calculated based on the assumption that Lyman α follows the same relative variation relationship to $F_{10.7}$ in August 1979 as it does between July 1977 and December 1978. The model is within the error bars for 13 out of 14 rocket measurements (there are no error bars for three rockets which made photographic observations).

Figure 7 shows the Feng et al. integrated spectrum for 5.0–57.5 nm in the same format as Figure 6. The modeled integrated EUV flux between 5.0 and 58.0 nm is overplotted. The model is within the error bars of 9 out of 14 rocket flights and is very close to one of the University of Southern

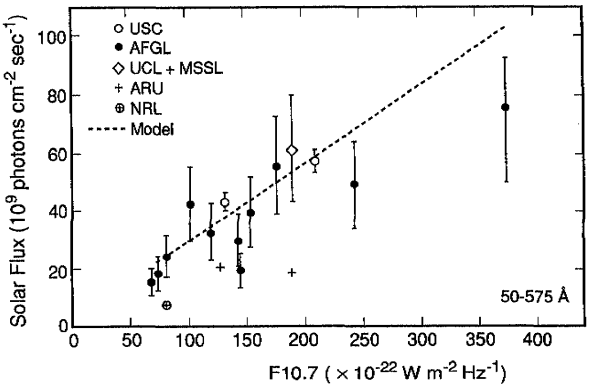

Fig. 7. The integrated solar EUV flux between 5.0 and 57.5 nm is taken from *Feng et al.* [1989] (points with error bars). The measurements are taken by the same organizations listed in the caption for Figure 6. The EUV model is represented as a dotted line and is described in the text. From Feng et al., all error bars on the measurements are ±30% except for the USC data, which are ±7%. The NRL and ARU photographic data have no error bars plotted.